Stoichiometry and Specificity of In Vitro Phosphopantetheinylation and Aminoacylation of the Valine-Activating Module of Surfactin Synthetase†

Paul H. Weinreb,‡ Luis E. N. Quadri,‡ Christopher T. Walsh,*,‡ and Peter Zuber§

Department of Biological Chemistry and Molecular Pharmacology, Harvard Medical School, Boston, Massachusetts 02115, and Department of Biochemistry and Molecular Biology, Louisiana State University Medical Center, Shreveport, Louisiana 71130

Received August 11, 1997; Revised Manuscript Received October 21, 1997

ABSTRACT: Surfactin synthetase is the enzyme responsible for biosynthesis of the lipoheptapeptide antibiotic surfactin by *Bacillus subtilis*. Fragments of SrfB1, the L-valine-activating module of the second subunit of surfactin synthetase, were overproduced in *Escherichia coli*. In addition to a 143-kDa SrfB1 fragment that contains four domains putatively involved in activation (adenylation domain), autoaminoacylation (peptidyl carrier protein (PCP) domain), and peptide bond formation (two condensation domains), subfragments comprising two domains (104-kDa condensation−adenylation and 73-kDa adenylation−PCP), and one domain (18-kDa PCP) were also overproduced in and purified from *E. coli* as N-terminal hexahistidine fusion proteins. Incubation of these domains with pure Sfp, a phosphopantetheinyl transferase (PPTase) from *B. subtilis*, and CoA allowed quantitation of posttranslational phosphopantetheinylation of Ser999 by mass spectrometry for the 18-kDa PCP fragment and by radioassay using cosubstrate [^{3}H] pantetheinyl-coenzyme A for all PCP-containing constructs. The phosphopantetheine stoichiometry correlated with the subsequent mole fractions of [^{14}C] valyl groups that could be covalently transferred to these holo-PCP domains. In turn, the catalytic efficiency of intramolecular aminoacylation of the 143-kDa fragment could be compared with the reaction "in trans" between adenylation and PCP fragments of SrfB1. The corresponding holo-PCP domain of the next module, SrfB2, was not detectably aminoacylated by SrfB1, indicative of protein−protein recognition between adenylation and cognate PCP domains. These results should permit future exploration of the timing and specificity of peptide bond formation by this class of biosynthetic enzymes.

A wide range of naturally occurring peptide-based compounds are synthesized enzymatically by the action of multifunctional nonribosomal peptide synthetases (*1*). These enzymes activate amino acid monomers first as tightly but noncovalently bound aminoacyl-AMP mixed anhydride species then as covalent amino acyl-thioester intermediates, where the thiol is provided by a 4′-phosphopantetheinyl (P-pant)[1] group introduced posttranslationally at a consensus serine site by a phosphopantetheinyl transferase (PPTase) (*2*). Peptide bond formation and growing chain translocation then occur between an amino acyl-S-P-pant domain and an adjacent peptidyl-S-P-pant domain. This "multienzyme thiotemplate" mechanism for peptide chain growth dictates that each amino acid-activating module must contain at least an adenylation domain and an adjacent peptidyl carrier protein (PCP) domain (*3*). In addition there are intermodule "condensation" (also called "elongation") domains, putatively involved in peptide bond formation, at each site of peptide chain extension, and epimerization domains wherever D-amino acids are incorporated. All of these domains are readily identifiable by the presence of highly conserved core sequences (*4*). Indeed the fungal enzyme cyclosporin synthetase, the largest enzyme characterized, contains over 15 000 amino acids in a single polypeptide with 11 recognizable amino acid activation modules, each with adenylation domains and adjacent consensus serine sites that mark PCP domains as well as condensation, epimerization, and N-methylation domains (*5*).

Although the first step (eq 1, left) in nonribosomal peptide synthetase action, the formation of aminoacyl-AMP, is classically and readily measured by amino acid-dependent [^{32}P]PP_i → ATP isotope exchange, the second step (eq 1, right) of amino acyl-S-enzyme formation and all subsequent steps have been more difficult to assay. In particular,

$$\mathrm{AA} + \mathrm{ATP} \underset{-PP_i}{\overset{\text{Enz-PPant-SH}}{\rightleftharpoons}} [\text{AA-AMP•Enz-PPant-SH}] \xrightarrow[-\mathrm{AMP}]{} \text{AA-S-PPant-Enz} \quad (1)$$

† This work was supported by National Institutes of Health Grants GM20011 (C.T.W.) and GM45898 (P.Z.). P.H.W. was supported by National Institutes of Health Postdoctoral Fellowship GM18721-01.

* Corresponding author e-mail, walsh@walsh.med.harvard.edu.

‡ Harvard Medical School.

§ Louisiana State University Medical Center.

[1] Abbreviations: ACV, 4-(L-2-aminoadipyl)-L-cysteinyl-D-valine; ACPS, holo-acyl carrier protein synthase; AMP, adenosine 5′-monophosphate; ArCP, aryl carrier protein; ATP, adenosine 5′-triphosphate; BSA, bovine serum albumin; CoA, coenzyme A; DEBS, 6-deoxyerythronolide B synthase; DTT, dithiothreitol; HPLC, high-pressure liquid chromatography; LSC, liquid scintillation counting; MALDI-TOF, matrix-assisted laser desorption time-of-flight mass spectrometry; PCP, peptidyl carrier protein; P-pant, 4′-phosphopantetheine; PP_i, inorganic pyrophosphate; PPTase, 4′-phosphopantetheinyl transferase; SDS, sodium dodecyl sulfate; TCA, trichloroacetic acid.

S0006-2960(97)01985-5 CCC: $15.00
Published on Web 01/23/1998

recombinant synthetases and synthetase domains exhibit low fractional stoichiometries of conversion from inactive apo-forms of PCP domains to active, phosphopantetheinylated holo-PCP domains, presumably due to the inability of the *E. coli* PPTases to effectively modify heterologous substrates (*6*, *7*).

We have recently identified a large family of PPTases that use coenzyme A (CoA) as the donor of the 4′-phosphopantetheinyl group in the modification of consensus serine residues (eq 2) (*8*). This family includes (a) holo-acyl carrier

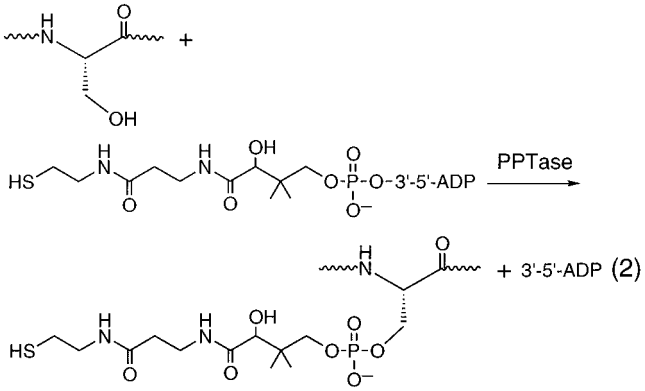

protein synthase (ACPS), which modifies the apo-ACP in *E. coli* fatty acid biosynthesis (*9*); (b) EntD, which modifies apo-EntB and apo-EntF in *E. coli* enterobactin synthesis (*8*, *10*); and (c) a set of peptide synthetase-selective PPTases, including Sfp for surfactin biosynthesis in *B. subtilis* (*8*, *11*), and Gsp for gramicidin biosynthesis in *B. brevis* (*12*).

The availability of PCP-selective PPTases now allows for mechanistic investigation of the steps involved in nonribosomal peptide synthesis, which can only proceed when apo-PCP domains have been converted to holo-PCP domains. As an example, we report here studies on one of the seven amino acid-activating modules in surfactin synthetase, namely, the SrfB1 module, which activates the fourth amino acid L-valine in the biogenesis of the lipoheptapeptide antibiotic surfactin (Figure 1). Surfactin, a powerful biosurfactant, is assembled by the four enzymes SrfA−D (Figure 2) where SrfA and SrfB each comprise three modules for recognition and incorporation of specific amino acids, SrfC activates the seventh amino acid, and SrfD (not shown) is proposed to possess thioesterase activity (*13*−*16*). The SrfB subunit of surfactin synthetase is a 401-kDa protein containing the modules SrfB1, SrfB2, and SrfB3, which activate Val, Asp, and Leu, respectively (Figure 2). We have expressed N-terminal hexahistidine fusions of the full-length SrfB1 module and several truncated constructs, including fragments corresponding to the adenylation and PCP domains, as substrates to investigate the rate and stoichiometry of phosphopantetheinylation and to assess the ability of these modified enzymes to undergo both intra- and intermolecular covalent aminoacylation.

EXPERIMENTAL PROCEDURES

Materials and Methods. *Bacillus subtilis* Sfp (*11*) was overproduced and purified as described in the accompanying paper (*17*). EntB ArCP was overproduced and purified by A. M. Gehring as previously described (*10*). TycA PCP (*18*) was a gift of M. Marahiel (Phillips-Universität Marburg).

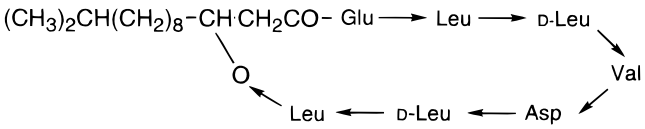

FIGURE 1: Structure of surfactin. Arrows indicate the orientation of the peptide backbone (N- to C-terminal).

[^{3}H]CoA was prepared as described and was used as the disulfide (*8*). The specific activity contained in the phosphopantetheine portion of the [^{3}H]CoA was estimated based on previous preparations to be 70% of the total activity. Other radiolabeled compounds were purchased from DuPont New England Nuclear.

Construction of E. coli Strains Expressing SrfB Domains and Mutant Derivatives. Plasmid pML118 (*8*) is a derivative of pPROEX-1 (Life Technologies) carrying a 3647-bp *Eco*RV fragment of *srfB* encoding the first amino acid-activating module (SrfB1) of the surfactin synthetase SrfB subunit. This plasmid has been shown (*8*) to direct the production of a 143-kDa, hexahistidine-tagged protein, H_6-SrfB1.143, containing amino acid residues 92−1307 of SrfB, which include the SrfB1 adenylation and thioesterification domains along with the intermodule regions believed to function in peptide bond formation.

Plasmid pZB1.104 is a pML118 derivative that has undergone a deletion of the PCP domain by cleavage of the plasmid with *Bgl*II (nucleotide position 2928 of *srfB*) and *Bam*HI, located within the multiple cloning site of the pPROEX-1 vector at the 3′-end of the insert, followed by intramolecular ligation. pZB1.104 directs the production of H_6SrfB1.104 containing the condensation motif upstream of SrfB1 and the SrfB1 adenylation domain.

Two mutant variants of pML118 were constructed by PCR amplifying the region of *srfB* corresponding to the *Eco*RV fragment that was used to construct the pML118 parent plasmid. The template DNA was isolated from strains LAB1295 (*srfBS999A*) (*19*) and from LAB1754 (*srfBD148A*) (*20*). The *srfBS999A* mutation eliminates the phosphopantetheinylation site of SrfB1, and the *srfBD148A* mutation removes a conserved residue from the first condensation domain. Oligonucleotides 1-F and 1-R (Table 1), spanning sequences 231−260 and 3908−3935 respectively, were used to PCR amplify the *srfB1* regions of LAB1295 and LAB1754. The PCR fragments were cleaved with *Eco*RV and ligated with *Stu*I cleaved pPROEX-1, yielding plasmids pML-118S999A bearing the *S999A* allele of *srfB* and pML118-D148A bearing the *D148A*, producing H_6SrfB1(S999A).143 and H_6SrfB1(D148A).143, respectively.

Plasmid pZW5 is a pPROEX-1 derivative that directs the expression of H_6SrfB1.73, a protein containing amino acids 462−1089 of SrfB including the adenylation and thioesterification domains of the SrfB1 module, but lacking the interdomain condensation regions encoded by plasmid pML118 and the mutant derivatives described above. The region of *srfB1* spanning nucleotides 1384−3263 of the *srfB* gene was amplified by PCR using the oligonucleotides 2-F and 2-R. The PCR product was cleaved with *Eco*R1 and *Xho*I and inserted into *Eco*R1 and *Xho*I cleaved pPROEX-1.

Plasmid pZB2.76, encoding H_6SrfB2.76, was constructed by first amplifying by PCR the sequence of the *srfB* gene extending from nucleotide 4338 to nucleotide 6285 using

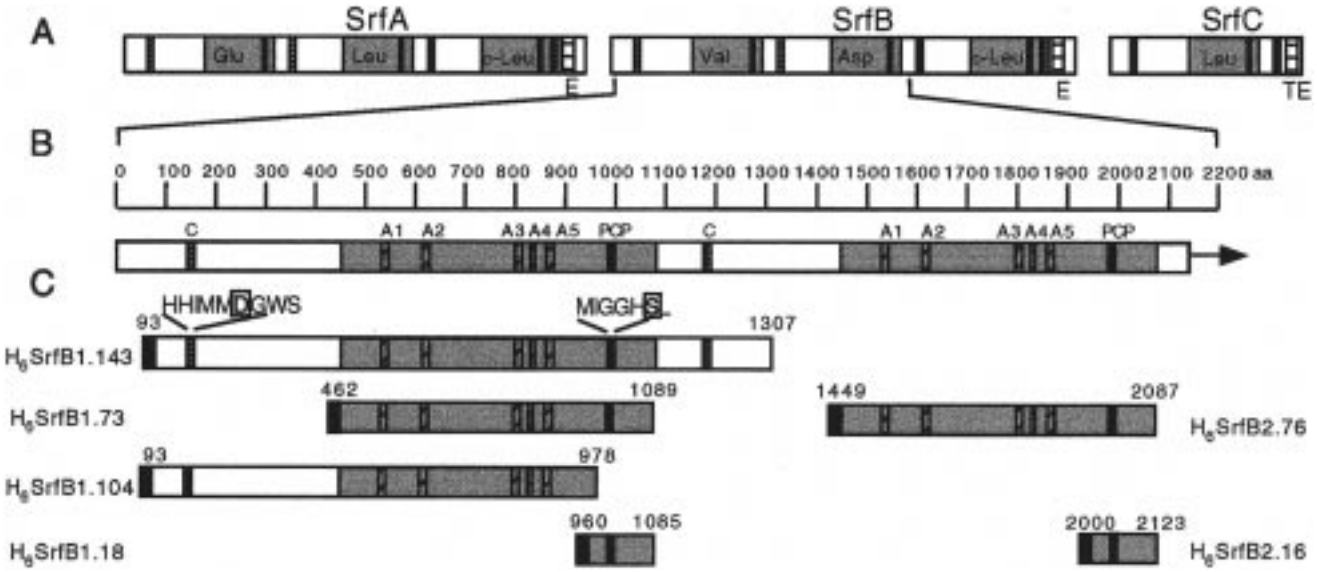

FIGURE 2: Schematic representation of surfactin synthetase and recombinant fragments. (A) The three component proteins SrfA, SrfB, and SrfC are indicated. The fourth component of surfactin synthetase, the putative thioesterase SrfD, is not shown. The positions of epimerase (E) and thioesterase (TE) motifs are indicated. (B) In the expanded view of the SrfB1 and SrfB2 modules, the positions of conserved sequences demarcating the condensation (C), adenylation (A1−A5), and peptidyl carrier protein (PCP) domains are indicated. (C) The fragments constructed in this work contain either one (H_6SrfB1.18 and H_6SrfB2.16), two (H_6SrfB1.104, H_6SrfB1.73, and H_6SrfB2.76), or four (H_6SrfB1.143) functional domains. The N-terminal hexahistidine tag (black box) and the two mutated residues, Asp148 and Ser999, are indicated. Numbering corresponds to the SrfB amino acid sequence.

Table 1: Plasmids and Oligonucleotide Primers for Cloning and Overproduction of Surfactin Synthetase Fragments

protein	plasmid	primers[a]
H_6SrfB1.143	pML118[a]	NA
H_6SrfB1.104	pZB1.104[b]	NA
H_6SrfB1(S999A).143	pML118S999A	1-F GGTCGTGTTAGCGGAACGCAAAACAAAAGT
		1-R CGAGCCGACAAT**GATATC**ATCCTGTGAC
H_6SrfB1(D148A).143	pML118D148A	1-F GGTCGTGTTAGCGGAACGCAAAACAAAAGT
		1-R CGAGCCGACAAT**GATATC**ATCCTGTGAC
H_6SrfB1.73	pZW5	2-F GCC**GAATTC**CTGAAGGAATGGCTGTTCACCAAGTGTTTG
		2-R GGC**CTCGAG**CAGAAGTACAGCGGGGACGTTGTAGCTT
H_6SrfB2.76	pZB2.76	3-F GAC**GGATCC**CGCCGCTGGAGCCGCCACTTTGT
		3-R CGG**CTCGAG**TACTTGATGGCCGCCTGAAACAGCA
H_6SrfB1.18	pZW6	4-F AGC**CATATG**TTGCAGCCGGAATACGCAGCACCAAAAA
		4-R CAG**AAGCTT**AACAGCGGGGACGTTGTAGCTTGTGTTTG
H_6SrfB2.16	pSRFB2.16	5-F CACAATCC**CATATG**AAGGCCTTGGCCGCACCGGAG
		5-R TCCA**AAGCTT**AAACAGATGGCATGTTGTAGCTTAT

[a] Ref 8. [b] Derived from pML118 (see Experimental Procedures). [c] NA, not applicable. The sequences in bold indicate restriction sites as specified in the text.

oligonucleotides 3-F and 3-R. The PCR fragment was cleaved with *Bam*HI and *Xho*I and inserted into *Bam*HI−*Xho*I-cleaved pPROEX-1.

Plasmid pZW6 directs the production of a hexahistidine-tagged version of the PCP domain of SrfB1. The product of pZW6, H_6SrfB1.18, contains the site of posttranslational phosphopantetheinylation but lacks the other active sites of the SrfB1 module. A region of *srfB* spanning nucleotides 2876−3254 was amplified by PCR using oligonucleotides 4-F and 4-R. The PCR fragment was cleaved with *Nde*I and *Hin*dIII and inserted into *Nde*I−*Hin*dIII-cleaved pPROEX-1.

Plasmid pSrfB2.16 similarly directs the production of a 16-kDa hexahistidine-tagged PCP domain of SrfB2. The region of SrfB spanning nucleotides 5984−6380 was amplified by PCR using oligonucleotides 5-F and 5-R. The PCR fragment was cleaved with *Nde*I and *Hin*dIII and inserted into *Nde*I−*Hin*dIII-cleaved pET28b (Novagen).

The ligation reactions described above were used to transform competent *E. coli* DH5α cells with selection for ampicillin (25 μg/mL, for pPROEX-1-based plasmids) or kanamycin (50 μg/mL, for pET28b-based plasmids). The resulting plasmids were introduced by transformation into competent cells of *E. coli* BL21(DE3) for the purpose of expressing plasmid insert DNA for the overproduction of H_6SrfB proteins.

Overproduction and Purification of SrfB Fragments. Cultures of BL21(DE3) harboring expression plasmids in 2× YT media containing ampicillin (100 μg/mL, for pPROEX-1-based plasmids) or kanamycin (50 μg/mL, for pET28b-based plasmids) were induced with isopropyl β-D-thiogalactopyranoside for 4 h at 37 °C (H_6SrfB1.18 and H_6SrfB2.16) or 25 °C (all others). Cells were harvested by centrifugation, resuspended in lysis buffer (5 mM imidazole, 500 mM NaCl, 0.1 mM phenylmethanesulfonyl fluoride, 20 mM Tris-HCl, pH 7.9), and lysed by two passages through a French press

at 16 000 psi. Cellular debris was removed by centrifugation at 15000*g* for 30 min. The soluble His_6-tagged proteins were purified using nickel-chelate chromatography on His-Bind resin (Novagen). Protein concentrations were determined using the colorimetric Bradford protein assay (Bio-Rad), with BSA as a standard.

ATP-[^{32}P]PP$_i$ Exchange Kinetics. ATP-pyrophosphate exchange was assayed as previously described (*6*) with minor modifications. The assay mixture contained 2 mM ATP, amino acid, and 50 nM enzyme in buffer A (10 mM $MgCl_2$, 25 mM dithiothreitol (DTT), and 75 mM Tris-HCl, pH 8.8). Exchange was initiated by addition of 1 μCi of sodium [^{32}P]-pyrophosphate (to 1 mM) in a total reaction volume of 0.1 mL. Kinetic experiments were performed under linear initial velocity conditions. After incubation at 37 °C for 10 min, the reaction was quenched by the addition of 0.5 mL of a charcoal suspension [1.6% (w/v) activated charcoal, 0.1 M tetrasodium pyrophosphate, 0.35 M perchloric acid]. The charcoal was pelleted by centrifugation, washed once with 1 mL of H_2O, resuspended in 0.5 mL of H_2O, and added to a scintillation vial containing 3.5 mL of scintillation fluid, and the bound radioactivity was determined by liquid scintillation counting (LSC).

Covalent Incorporation of [^{3}H]Phosphopantetheine. The incorporation of [^{3}H]CoA was performed as described (*8*) in an assay mixture containing 40 μM [^{3}H]CoA disulfide (96 Ci/mol specific activity), 5 μM substrate, and 650 nM Sfp in 0.1 mL of buffer A. To determine total incorporation of [^{3}H]phosphopantetheine, reactions were incubated at 37 °C for at least 1 h, quenched with 0.8 mL of 10% TCA and 0.375 mg BSA (as a carrier), pelleted by centrifugation, washed three times with 10% TCA, solubilized in 1 M Tris base, added to 3.5 mL of liquid scintillation fluid, and quantified by LSC.

HPLC and Mass Spectrometry. HPLC and MALDI-TOF data on holo-H_6SrfB1.18 were acquired using crude phosphopantetheinylation reaction mixtures performed under conditions identical with those described above, except that unlabeled CoA was used in place of [^{3}H]CoA disulfide. Analytical HPLC was performed using a Vydac C18 reversed-phase column (4.6 mm × 25 cm) on a Waters 600 HPLC system with monitoring at 220 nm. Samples (10−20 μg of protein) were eluted at 0.5 mL/min using a linear gradient from 40% to 74% of 2-propanol in 0.1% trifluoroacetic acid. MALDI-TOF mass spectrometry was performed at the Howard Hughes Medical Institute Biopolymers Facility, Harvard Medical School.

Covalent Incorporation of [^{14}C]Val or [^{3}H]Val. For reactions "in cis", substrates were first phosphopantetheinylated using Sfp in a 0.1-mL reaction using unlabeled CoA in place of [^{3}H]CoA disulfide. After incubation for 1 h, 10 mM ATP and 540 μM (0.5 μCi) [^{14}C]Val (8.1 Ci/mol) were added to make a total reaction volume of 0.11 mL. After incubation for 20 min at 37 °C, the reaction was quenched with TCA and treated as described above, with quantification by LSC.

For reactions "in trans", a mixture of the substrate PCP (10 μM) and the H_6SrfB1(S999A).143 mutant (4 μM) was incubated with 96 μM CoA and 650 nM Sfp in a total volume of 0.1 mL of buffer A for 1 h at 37 °C. To this was added 250 μM [^{3}H]Val (36 Ci/mol) and 10 mM ATP to make a total reaction volume of 0.11 mL, which was incubated at 37 °C for 30 min prior to quenching.

Samples for autoradiography were quenched without using BSA as a carrier, and pellets were solubilized in SDS sample buffer titrated with 1 M Tris base. Samples were resolved using 4−20% gradient gels (BioRad), stained with Coomassie Blue, soaked for 20 min in Amplify (Amersham), dried at 80 °C under vacuum, and exposed to X-ray film for 192 h at −70 °C.

Kinetics of Amino Acid Incorporation. A reaction mixture containing H_6SrfB1.143 (for the in cis assay) or H_6SrfB1.18 (for the in trans assay), Sfp, and CoA in buffer A was incubated at 37 °C for 1 h to ensure complete phosphopantetheinylation (concentrations indicated in figure legends). Aminoacylation was initiated by the addition of [^{3}H]Val and ATP (for the in cis assay) or [^{3}H]Val, ATP, and H_6SrfB1.104 (for the in trans assay), and samples were quenched at regular intervals using the aforementioned TCA precipitation protocol and quantitated using LSC. Substrate vs velocity measurements were performed under linear initial velocity conditions.

Kinetics of [^{14}C]Val-SrfB1 Thioester Decomposition. H_6-SrfB1.143 (10 μM) was incubated with 96 μM CoA and 650 nM Sfp in 0.2 mL of buffer A for 1 h at 37 °C. To this was added ATP (to 2 mM) and 1 μCi [^{14}C]Val (to 16 μM), and the reaction was incubated at 37 °C for 30 min further. To remove excess valine and ATP and to adjust the pH, the reaction was passed through a Bio-Spin 6 (Bio-Rad) desalting column preequilibrated in 20 mM sodium phosphate buffer, pH 6.5−8.5. At regular time intervals, aliquots (22 μL) were quenched with TCA and quantitated as above.

RESULTS

SrfB1 Constructs, Expression, and Overproduction. The SrfA and SrfB multicatalytic proteins are large, each of approximately 400 kDa. The position of SrfB1, the first amino acid-activating module in SrfB, can be defined based on sequence homology (*4*, *21*) to comprise an adenylation domain of approximately 500 amino acid residues and a PCP domain of 80 residues and is preceded and followed by condensation domains of 350 residues each that may catalyze peptide bond formation (e.g., acyl-Glu-Leu-D-Leu→Val and acyl-Glu-Leu-D-Leu-Val→Asp, respectively) (Figure 2). We have designed a 143-kDa fragment comprising the adenylation, PCP, and both condensation domains (residues 93−1307) of SrfB (*8*). This maximal SrfB1 module could be heterologously expressed as an N-terminal hexahistidine-tagged construct (H_6SrfB1.143) in soluble form in *E. coli*. The H_6SrfB1(D148A).143 construct was also produced by cloning and expressing in *E. coli* a PCR-amplified fragment encoding the 143-kDa derivative from a *B. subtilis* strain containing a mutation of a conserved aspartate in the first condensation domain of SrfB1, which abolishes surfactin production in vivo (*20*). The DNA encoding the H_6SrfB1-(S999A).143 mutant, with a mutation in the PCP domain of the consensus Ser for phosphopantetheinylation by the PPTase Sfp, was also amplified from the corresponding mutant strain (*19*) for use in in trans aminoacyl transfer assays since it should be incompetent for covalent autoaminoacylation (*22*). To the same end, we also constructed H_6-SrfB1.104, a deletion of the 143-kDa construct that lacks

the PCP and downstream regions and comprises only the adenylation domain and the upstream condensation domain.

In addition to the four-domain-containing 143-kDa fragment of SrfB1, the 73-kDa two-domain fragment H_6SrfB1.73 was constructed spanning residues 462−1089 of SrfB, which should represent the minimal SrfB1 valine-activating module containing an autonomously folding adenylation domain specific for Val and the downstream intramolecular PCP domain for covalent docking of Val. An analogous 76-kDa fragment of the next module SrfB2 (H_6SrfB2.76) was similarly constructed, produced, and purified. Finally for experiments in which we proposed to study the recognition and efficiency of PCP domains supplied in trans to adenylation domains (vide infra), PCP domains of SrfB1 (H_6SrfB1.18) and SrfB2 (H_6SrfB2.16) were also prepared and purified. All of these fragments could be overexpressed as soluble proteins and purified using Ni affinity chromatography to provide SrfB fragments in predominantly (>90% as determined by [^{3}H]CoA incorporation) the apo-form.

Posttranslational Phosphopantetheinylation of Apo-Forms of SrfB1 PCP-Containing Fragments by Sfp. While it was not expected that the apo or holo status of PCP domains would likely affect the first step of amino acid activation, aminoacyl-AMP formation, it was clear that no formation of the covalent amino acyl-S-PCP domains, held to be prerequisite for subsequent peptide bond formation, could occur unless apo-PCP domains were converted to holo-PCP domains in the various 18-, 73-, and 143-kDa constructs of SrfB1. To this end, we had previously reported overproduction of the surfactin synthetase modifying enzyme Sfp and proved its catalytic capacity as a PPTase using H_6SrfB143 and other heterologous apo-PCP-containing substrates (*8*). In the accompanying paper, we outline the determinants of catalytic efficiency and recognition by Sfp (*17*). For this study, it was important to prove unambiguously that phosphopantetheinylation occurred when proteins containing apo-PCP domains were incubated with Sfp.

The apo to holo conversion of the SrfB1 substrates using purified Sfp was monitored by several independent methods. For the relatively small H_6SrfB1.18 domain, we were able to monitor the conversion using mass spectrometry. MALDI-TOF mass spectrometry of the H_6SrfB1.18 fragment gave a molecular ion at 18063 Da, close to the calculated value of 18077 Da (Figure 3). Following incubation with Sfp, the mass spectrum indicated conversion to a molecular ion at 18420 Da, compared to the calculated value of 18417 Da for covalent incorporation of a phosphopantetheine group. Minor components corresponding to either proteolytic or mass spectral fragments were also observed and showed complete conversion to holo-forms (data not shown). This and subsequent reactions were carried out under reducing conditions in order to prevent the formation of disulfide-containing oxidized byproducts.

The fractional stoichiometry of modification is a critical issue for all subsequent evaluations of aminoacylation stoichiometry, as will be discussed below, and has been a serious problem in the field when heterologous expression of functional peptide synthetases has been attempted in the past (*6, 23*). Incubation of the apo-form of H_6SrfB1.18 with Sfp led to quantitative conversion to a new chromatographic form on HPLC (Figure 3) as well as conversion to the holo-phosphopantetheinylated form by mass spectrometry.

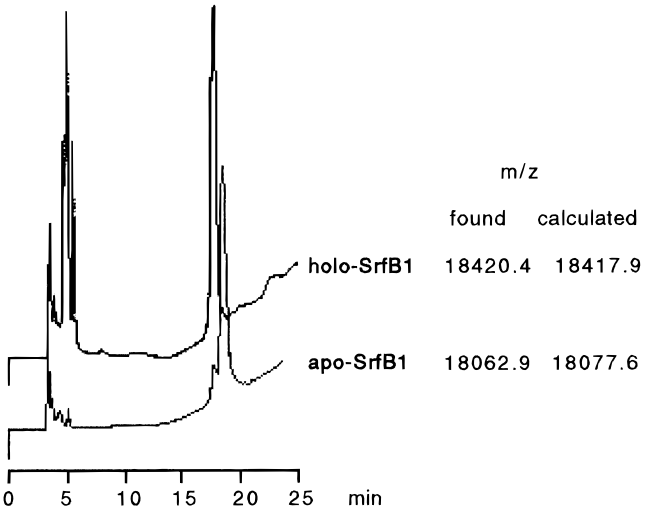

FIGURE 3: HPLC of apo- and holo-H_6SrfB1 PCP domains. Lower trace, purified H_6SrfB1.18; upper trace, holo-H_6SrfB1.18 reaction mixture. Retention times for apo- (lower) and holo-H_6SrfB1.18 (upper) were 18.4 and 17.7 min, respectively. A co-injection of the two samples indicated two distinct peaks (data not shown). A small amount (<15%) of the recombinant PCP domain is modified in vivo by heterologous *E. coli* PPTase activity (observed at 17.7 min in lower trace).

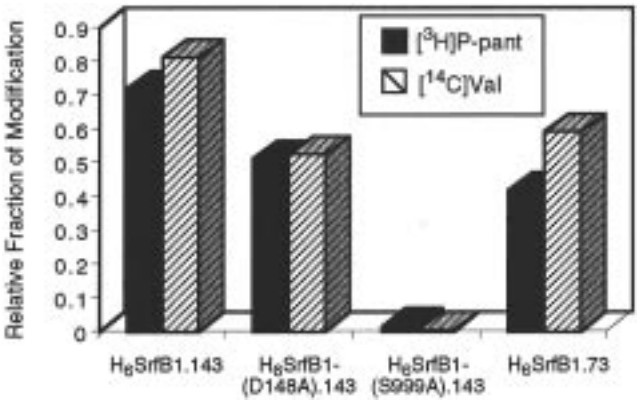

FIGURE 4: Covalent incorporation of [^{3}H]phosphopantetheine and [^{14}C]Val into SrfB1 fragments. Incorporation of [^{3}H]phosphopantetheine (solid bars) and [^{14}C]Val (hatched bars) into the wild-type and mutant full-length SrfB1 constructs was monitored by radioassay. The S999A mutant was not modified, supporting the presence of a single, highly specific phosphopantetheinylation site. The degree of modification was calculated relative to H_6SrfB1.18, which was shown by HPLC and mass spectrometry to be quantitatively phosphopantetheinylated. The extent of covalent aminoacylation mirrored the phosphopantetheine stoichiometry, indicative of complete valinylation of holo-SrfB1.

An alternative method of quantifying the apo to holo conversion was to measure the incorporation of [^{3}H]-phosphopantetheine from [^{3}H]CoA into the substrate using a TCA precipitation assay. This method was used to analyze the stoichiometry of modification of the apo-forms of the 73- and 143-kDa two- and four-domain SrfB1 constructs as well as to confirm the quantitative conversion of the apo-H_6SrfB1.18 construct demonstrated by mass spectrometry and HPLC. As shown in Figure 4, the wild-type 143-kDa SrfB1 fragment and the corresponding D148A mutant were covalently modified, as were the 73- and 18-kDa SrfB1 PCP-containing constructs. The H_6SrfB1S999A.143 mutant showed no incorporation of tritium relative to controls, consistent with Ser999 being the unique site of posttranslational

Table 2: Measured Values of K_m and k_{cat} for SrfB1 Enzymes in the L-Valine-Mediated ATP/PP_i Exchange Reaction

enzyme	K_m (mM)	k_{cat} (min^{-1})	k_{cat}/K_m (mM^{-1} min^{-1})
H_6SrfB1.143	9.2	432	47
holo-H_6SrfB1.143	5.2	173	33
H_6SrfB1(D148A).143	12.4	377	30
H_6SrfB1(S999A).143	4.9	230	47
H_6SrfB1.104	5.3	320	60
H_6SrfB1.73	22.7	22.6	1.0

modification. Because HPLC analysis indicated complete modification of the H_6SrfB1.18 substrate, we were able to calibrate the specific radioactivity of [^{3}H]CoA prepared by tritium gas exposure of unlabeled CoA. Assignment of the radioactivity transferred by Sfp to apo-H_6SrfB1.18 as 1.0 equiv allowed us to quantify stoichiometries ranging from 0.4 to 0.9 for the 143- and 73-kDa substrates (Figure 4). Variation in the stoichiometry of phosphopantetheinylation as assessed by the recovery of ^{3}H-labeled products most likely arises from incomplete recovery of radiolabeled proteins in the TCA precipitation step, variations in protein homogeneity, and/or experimental errors in the determination of protein concentration by colorimetric methods referenced to BSA.

Catalytic Efficiency and Specificity for Amino Acyl-AMP Formation. An initial catalytic test of constructs containing the proposed adenylation domain of SrfB1 was amino acid-dependent exchange of [^{32}P]PP_i into ATP, reflecting reversible formation of the tightly bound amino acyl-AMP from which PP_i dissociates. As shown in Table 2, the apo-H_6-SrfB1.143 full-length module had a k_{cat} of 432 min^{-1} and a K_m for L-valine of 9.2 mM. The k_{cat} and K_m were essentially unaffected by the phosphopantetheinylation status of the 143-kDa protein, consistent with the expectation that the PCP domain is a separate folding entity from the adenylation domain and has no influence on the adenylation step. Consistent with this interpretation was the observation (Table 2) that the S999A 143-kDa mutant protein was effectively as efficient a valyl-AMP synthetase as H_6SrfB1.143 by this assay. Likewise, an equivalent k_{cat}/K_m was observed for the H_6SrfB1(D148A).143 mutant that cannot carry out peptide bond formation when in a full-length SrfB polypeptide context (*20*). The lack of a PCP domain in H_6SrfB1.104 had no effect on adenylation activity. In all of these experiments, the K_m for L-valine was in the millimolar range, in contrast to high micromolar K_m values reported for other adenylation domains of nonribosomal peptide synthetases (*24*, *25*). As anticipated, the SrfB1 construct(s) do not utilize aspartic acid, the substrate for the next SrfB2 module to support [^{32}P]PP_i→ATP exchange (data not shown and ref *8*).

The minimal activating modules H_6SrfB1.73 and H_6-SrfB2.76 showed a marked decrease in catalytic efficiency relative to the longer, 143-kDa counterparts. While still able to catalyze ATP−PP_i exchange, the K_m for Val of the H_6-SrfB1.73 construct was 2−3 times higher than that for the full-length module, and the k_{cat} was reduced by an order of magnitude (Table 2). The exchange catalyzed by the H_6-SrfB2.76 construct could not be saturated even up to 100 mM Asp (data not shown), consistent with the possbility that these constructs lack an important region for optimization of amino acid binding.

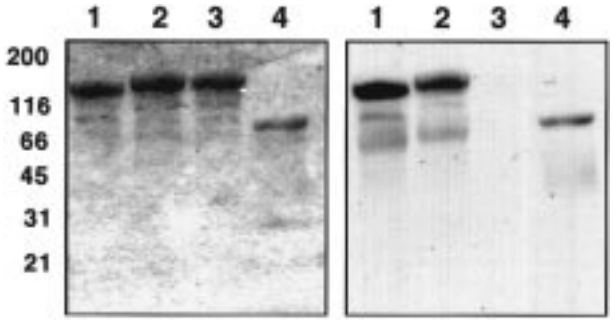

FIGURE 5: Coomassie stained gel (left) and autoradiogram (right) of [^{14}C]Val-labeled substrates. Phosphopantetheinylated proteins were incubated with [^{14}C]Val and ATP, quenched and loaded onto a 4−20% gradient SDS−polyacrylamide gel, and exposed to film, as described in the Experimental Section. Lane 1, H_6SrfB1.143; lane 2, H_6SrfB1(D148A).143; lane 3, H_6SrfB1(S999A).143; lane 4, H_6SrfB1.73.

Covalent Aminoacylation Stoichiometry in SrfB1 143- and 73-kDa Fragments. Once the PCP domains had been converted from apo- to holo-form, the phosphopantetheinylated 73- and 143-kDa SrfB1 fragments could be assessed for the ability to undergo covalent intramolecular aminoacylation. The apo-forms were first incubated with unlabeled CoA and Sfp under conditions identical with those under which [^{3}H]CoA incorporation was measured. Following addition of ATP and [^{14}C]Val, covalent loading was assessed by the TCA precipitation method. As shown in Figure 4, the aminoacylation stoichiometry parallels the phosphopantetheinylation stoichiometry. All molecules loaded with phosphopantetheine can be thioesterified by [^{14}C]Val-AMP generated in the adjacent intramolecular adenylation domain. A minor amount (<10%) of [^{14}C]Val incorporation was observed in the absence of Sfp (data not shown); this is presumably due to a small percentage of holo-protein produced by heterologous *E. coli* PPTase activity (*8*). No difference in stoichiometry between the H_6SrfB1.73 and the H_6SrfB1.143 fragments was observed. As expected, the H_6-SrfB1(S999A).143 cannot be aminoacylated as a consequence of not being phosphopantetheinylated. Autoradiography of the [^{14}C]valinylated 73- and 143-kDa fragments after SDS gel electrophoresis validated covalent labeling (Figure 5). No aminoacylation of holo-SrfB1 substrates with [^{14}C]-Asp (the substrate amino acid for SrfB2) was observed (data not shown). These results establish the quantitation needed for analysis of subsequent steps in these multicatalytic, multidomain peptide synthetases.

H_6SrfB1(S999A).143 and H_6SrfB1.104 Specifically Catalyze Aminoacyl Transfer in Trans to the PCP Domain of H_6SrfB1.18. The S999A mutant of SrfB1, which could not be modified with phosphopantetheine, was incompetent at intramolecular in cis autoaminoacylation. This allowed us the opportunity to investigate the aminoacylation of PCP domains in trans, using separate adenylation and PCP proteins (Figure 6).

H_6SrfB1(S999A).143 effectively transaminoacylated H_6-SrfB1.18 with [^{3}H]Val, as shown in Table 3. In this reaction, [^{3}H]Val is converted to [^{3}H]Val-AMP in the adenylation site of the adenylating fragment and is then transferred intermolecularly to the separate PCP fragment (Figure 6). Transfer requires prior conversion of the apo-form of H_6-SrfB1-PCP to the holo-form by Sfp and CoA.

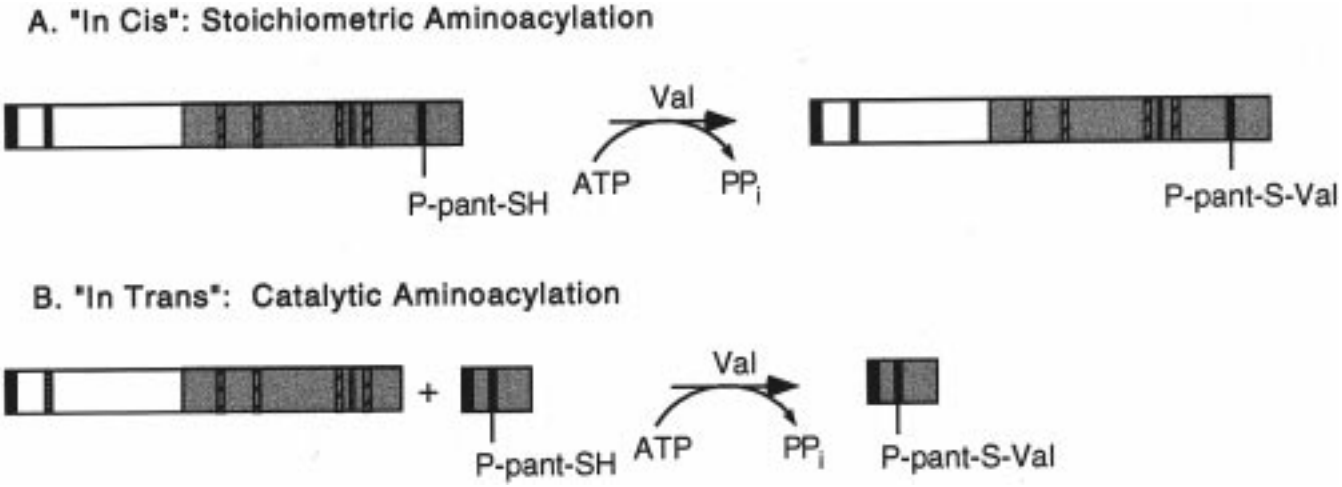

FIGURE 6: Model for intramolecular in cis vs intermolecular in trans aminoacylation of SrfB substrates. In panel A, which corresponds to the natural biosynthetic mechanism, equimolar amounts of enzyme and substrate amino acid are utilized in the autoaminoacylation process. In panel B, the adenylating enzyme is used to aminoacylate the corresponding holo-PCP domain with multiple catalytic turnovers. In the case of SrfB1, the transaminoacylation is selective for the corresponding substrate PCP domain.

Table 3: Incorporation of [^{14}C]Val into PCPs Using H_6SrfB1(S999A).143 in trans[a]

substrate PCP	[^{3}H]Val (pmol)
H_6SrfB1.18	131.9
H_6SrfB1.18 (−ATP)	4.2
H_6SrfB2.18	7.2
TycA PCP	1.5
EntB ArCP	1.4

[a] Reaction conditions: 300 μM CoA, 10 μM (1 nmol) substrate PCP, 4 μM H_6SrfB1(S999A).143, 650 nM Sfp; followed by 10 mM ATP, 250 μM Val (36 Ci/mol).

To address the specificity of the transaminoacylation reaction for the PCP component, the holo-PCP domain from SrfB2 (H_6SrfB2.16), which normally would be loaded with aspartic acid, was tested as a substrate for H_6SrfB1-(S999A).143-catalyzed transaminoacylation with [^{3}H]valine. As shown in Table 3, H_6SrfB2.16 showed no detectable labeling, revealing a clear specificity against the heterologous PCP domain. Also shown in Table 3 are two additional heterologous carrier protein domains, a 98 amino acid C-terminal fragment of the aryl carrier protein holo-EntB (EntB ArCP) (*10*) and a 115 amino acid PCP fragment from tyrocidine synthetase A (TycA) (*18*). As with SrfB2, neither holo-carrier protein functioned as a phosphopantetheinyl acceptor for valyl-AMP at the adenylation site of SrfB1. The H_6SrfB1.104 enzyme exhibited a comparable specificity for transfer to the cognate PCP substrate.

Kinetics of Aminoacylation in Cis vs in Trans. A comparison of the intra- and intermolecular aminoacyl transfer (in cis and in trans, respectively) was undertaken in order to obtain a measure of the importance of covalent tethering of adenylation and PCP domains. The intramolecular process involves rate constants for two successive reactions: the formation of Val-AMP and then transfer to form the thioester link in the holo-PCP domain. The $t_{1/2}$ for the process was determined to be 25 s, corresponding to a rate constant of 0.028 s^{-1} (Figure 7A). Given a k_{cat} of 432 min^{-1} for Val-AMP formation, the k of 0.028 s^{-1} most likely represents the Val-S-PCP formation rate including both the physical movement from adenylation domain to adjacent PCP domain and the acyl transfer chemical step. Since H_6-SrfB1.143 is both substrate and catalyst for its own modification, a K_m value was not determined. The valine dependence of product formation did allow computation of a K_d value of 3 μM.

The kinetics of aminoacylation in trans were then investigated in order for comparison to the natural intramolecular transfer reaction. Initial kinetic analysis of transaminoacylation of the H_6SrfB1.18 substrate with [^{3}H]Val by the H_6-SrfB1(S999A).143 mutant indicated that the K_m for the holo-PCP substrate was greater than 40 μM. The possibility existed that the S999A PCP product associated with the adenylating enzyme was competing effectively as an inhibitor against transfer to the external PCP fragment. Therefore, the H_6SrfB1.104 construct lacking the PCP domain was used to catalyze transaminoacylation to external holo-PCP domains. As shown in Figure 7B, there is a linear rate of increase of aminoacylation of H_6SrfB1.18 with no indication of saturation even by 90 μM, the highest concentration attainable in these experiments, suggesting a high K_m for the autologous holo-PCP domain when presented in trans. No difference between the S999A mutant and the truncated adenylation domain was observed, suggesting that the presence of the mutant PCP domain has no effect on the transfer reaction.

Stability of the [^{14}C]Val-S-P-pant Linkage. As a prelude to assessing the ability of the aminoacylated SrfB1 module to act either as an acceptor (from Leu-SrfA3) or as donor (to Asp-SrfB2) in peptide bond formation with adjacent aminoacylated modules, the stability of the base labile aminoacyl thiolester linkage of Val-P-pant-H_6SrfB1.143 was determined using [^{14}C]Val-labeled enzyme. At 25 °C and pH 6.5, the $t_{1/2}$ for thioester decomposition was about 100 min, dropping to ~40 min at pH 7.5 and to ~30 min at pH 8.5. It is anticipated that deprotonation of the valyl amino group will be catalyzed by SrfB1 [e.g., by side chains in the condensation domain (*4*)], so a basic pH optimum for interdomainal peptide bond formation may be expected.

DISCUSSION

The nonribosomal peptide synthetases, fatty acid synthases, and polyketide synthases have in common the task of iterative

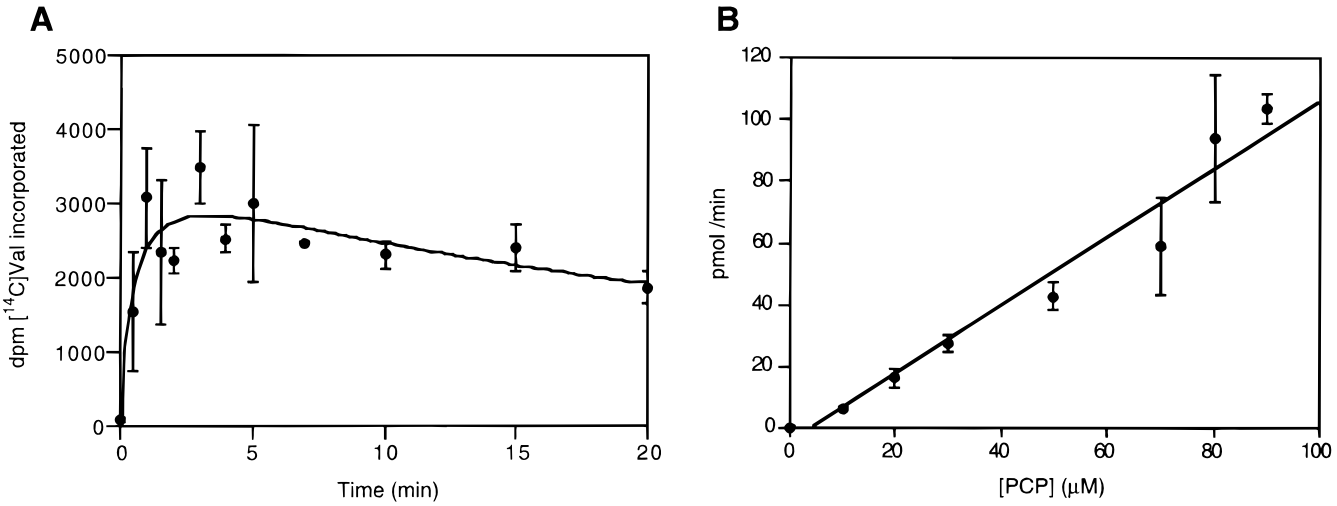

FIGURE 7: Kinetics of aminoacylation of SrfB1 PCP domains in cis and in trans. (A) Time course of [^{3}H]Val incorporation into holo-H_6-SrfB1.143 [200 μM CoA, 650 nM Sfp, 4 μM H_6SrfB1.143, 10 mM ATP, 250 μM [^{3}H]Val (167 Ci/mol)]. The $t_{1/2}$ determined from this assay is 25 s. (B) Plot of substrate concentration vs reaction velocity for H_6SrfB1.104-catalyzed incorporation of [^{3}H]Val into H_6SrfB1.18 [500 μM CoA, 650 nM Sfp, 330 nM H_6SrfB1.104, 10 mM ATP, 5 mM [^{3}H]Val (7.8 Ci/mol)].

addition of substrate monomer units to a growing chain that is covalently tethered during catalysis. Typically these are large catalysts with multiple domains fused into a single polypeptide or sets of multicatalytic subunits. Mechanistically, the polyketide synthases that make macrolide antibiotics such as erythromycin and the nonribosomal peptide synthetases are also united by processive transfer of the growing chain as a set of acyl (aminoacyl, peptidyl)-S-enzyme intermediates, as the elongating acyl chain is transferred from one posttranslationally introduced phosphopantetheinyl thiol unit to the next. Thus, ACV synthetase in penicillin biogenesis has three PCP domains (*26*), and cyclosporin synthetase is predicted to have 11 phosphopantetheine groups attached to 11 PCP domains (*5*). To dissect the mechanism, selectivity, and directionality of these multicatalytic synthases, it is essential to be able to control and determine the functional competence of each domain. In this work, we have focused on the quantitation of phosphopantetheinylation and subsequent aminoacylation of a single domain of surfactin synthetase, the enzyme responsible for production of the lipoheptapeptide surfactin in *B. subtilis*.

We focused on SrfB1, the first module of the three module SrfB enzyme, which activates and incorporates Val_4, Asp_5, and D-Leu_6 into the cyclic lipoheptapeptide antibiotic surfactin from *B. subtilis*. In part this devolves because of a prior knowledge base including the finding that Sfp is a Srf-modifying PPTase (*8*) and in part because the SrfB1 module is at the N-terminus of SrfB, possessing three proposed domains: for condensation (peptide bond formation: D-Leu_3→Val_4), aminoacylation (for Val-AMP formation), and thioesterification [PCP, the covalent aminoacylation site (Val-S-P-pant-Ser999)]. Although the boundaries of each domain must be defined somewhat arbitrarily, recent detailed sequence analyses (*4*, *18*, *21*, *27*) have defined more accuately the positions of the condensation, adenylation, and PCP domain consensus sequences. On the basis of these analyses, the condensation domains on either side of the SrfB1 module encompass the signature HHxxxDG motif (at positions 143−149 and 1182−1188), the adenylation domain comprises residues 491−948, and the PCP domain surrounds the xGG-(D/H)SL phosphopantetheinylation site (residues 995−1000). We therefore designed a four-domain 143-kDa polypeptide comprising residues 93−1307, which turned out to be soluble and readily purifiable when expressed as an N-terminal hexahistidine fusion construct in *E. coli*. Likewise the two mutant forms D148A and S999A were soluble as were the two-domain 73-kDa constructs and the one-domain 18-kDa PCP construct, setting the stage for analysis of posttranslational modification.

Assessment of the structural and functional integrity of peptide synthetase fragments containing multiple domains required an assay for each function. The three domain H_6-SrfB1.143 fragment should activate valine as Val-AMP in the adenylation domain; this was readily assayed by the valine-dependent [^{32}P]PP_i→ATP exchange assay. A k_{cat} of 300−400 min^{-1} was a robust indicator of adenylation domain function although the value of K_m (ca. 10 mM) is higher than expected. The decrease in catalytic efficiency in the two domain (73 and 76 kDa) constructs for both SrfB1 (Val activation) and SrfB2 (Asp activation) suggests these fragments may not fold to a fully native conformation and are a quantitative caveat. To study the function of the other two domains, the PCP domain (for covalent autoaminoacylation) and the condensation domains (catalysis of peptide bond formation between two adjacent aminoacylated PCP domains) requires substantial and quantifiable conversion from apo- to holo-PCP domains with stoichiometric posttranslational P-pant addition.

Prior studies had suggested that heterologous expression of peptide synthetase modules in *E. coli* led to very low mole fractions of posttranslational modification (*6*, *23*). We have elsewhere shown that the constitutive PPTase in *E. coli*, ACPS, will not modify apo-PCP domains (*8*), and indeed the H_6SrfB1.18 overproduced in *E. coli* was predominantly (>90%) in the apo form by HPLC mobility and subsequent mass spectrometric analysis. Therefore, the tritum label covalently introduced by pure Sfp acting as a PPTase with [^{3}H]CoA into the 18 kDa and, by extension, the 73- and 143-kDa SrfB1 fragments measures total holo-forms produced. By HPLC and mass spectrometric analysis of the H_6SrfB1.18 PCP domain fragment, quantitative conversion of apo to holo

was attainable. [^{3}H]CoA and TCA precipitation assays indicated similar levels of modification of the 143- and 73-kDa substrates. In any case, it is clear that the precipitation assay is not ideally suited for quantitation of modification stoichiometries without a correction/calibration by HPLC and mass spectrometry, as we have done for the PCP fragment.

Subsequent aminoacylation of the holo-PCP domains in 18-, 73-, or 143-kDa contexts, in trans as well as in cis, gave excellent stoichiometric correspondence, proving that Sfp can phosphopantetheinylate Ser999 in all three constructs and that the Val-AMP intermediate is quantitatively transferred to the cysteamine thiol terminus of the P-pant group. These data place the autoaminoacylation chemistry of eq 2 on a firm quantitative footing and should be a generalizable standard for any nonribosomal peptide synthetase study involving PCP domains, provided one has available the PPTase that recognizes its partner apo peptide synthetase. We anticipate that the *B. subtilis* Sfp may have broad enough specificity to recognize many apo-PCP domains, as evidenced by its ability to modify other SrfB PCP domains (e.g., H_6SrfB2.16) (*17*) as well as apo-EntB, apo-TycA, and apo-ACP (*8*).

Two aspects of eq 2, the transfer of the activated valyl group from Val-AMP sequestered in the adenylation domain of SrfB1 were further pursued. First was the demonstration of in trans or intermolecular transfer between fragments, and the second was an initial estimate of any specificity for aminoacyl transfer between apposite adenylation and PCP domains. In intact peptide synthetases, the transfer is in cis between domains within a multicatalytic subunit (e.g., SrfB1 to SrfB2) but is in trans when the growing peptide chain is passed between subunits (e.g., SrfA3 to SrfB1). The in trans thioesterification provides the opportunity to distinguish between catalytic and substrate determinants by separating the catalytic component (in the adenylation domain) from the substrate (the PCP domain). Incubation of equimolar amounts of adenylation and PCP domains of TycA has been shown to lead to an equivalent amount of phenylalanine incorporation as the undissected enzyme (*18*). However, nothing is currently known about comparative kinetics and selectivity of the two types of transfer.

The in cis thiolation of the [^{14}C]Val moiety to make [^{14}C]Val-S-P-pant-H_6SrfB1.143 was readily monitored by TCA precipitation and gave a $t_{1/2}$ of 25 s [k of 0.028 s^{-1} (1.8 min^{-1})] at pH 8.8 and 37 °C. A literature comparison exists for valine activation by the GS2 subunit of gramicidin S synthetase where a $t_{1/2}$ of 12 s at pH 7.2 and 30 °C was estimated (*28*). To assess in trans thiolation with the corresponding domains of SrfB1, two constructs were utilized. The H_6SrfB1(S999A).143 fragment is incompetent for conversion from apo- to holo- PCP form and is thus unable to autoaminoacylate. It cannot function in its normal in cis mode. It does, however, activate [^{14}C]Val as [^{14}C]-Val-AMP and then transfer it to the 18-kDa PCP fragment. The affinity of the adenylating enzyme for the PCP fragment was not high (K_m > 50 μM), and solubility limits prevented saturation.

To remove the potential complication of intramolecular competition by the apo-PCP domain in the H_6SrfB1-(S_{999}A).143 mutant fragment, the PCP domain was deleted entirely in the H_6SrfB1.104 fragment, which could still transfer [^{14}C]Val-AMP intermolecularly to the autologous PCP domain. Again the affinity for the cognate PCP was low, and saturation was not achieved at up to 90 μM H_6-SrfB1.18 acceptor. A k_{cat} of at least 8 min^{-1} was estimated for this catalytic thioesterification process.

Despite the apparent low affinity of SrfB1 condensation/adenylation domains for the autologous PCP domain, there was clear-cut evidence of selectivity. Most notable was the absence of detectable valyl transfer to holo-SrfB2 PCP domain (fully phosphopantetheinylated by Sfp). Nor did we observe aminoacyl transfer to holo-PCP thiol groups in a *B. brevis* TycA PCP domain or an *E. coli* EntB ArCP domain (Table 3). This suggests that there is some substantial degree of protein−protein recognition between an adenylation domain and the downstream intramolecular PCP domain to which aminoacyl transfer is directed. Given the physiological *inter*molecular transfer between SrfA3 and SrfB1, it may be instructive to look at heterologous recognition between adenylation and PCP domains in this pair.

The second type of study that should be enabled by the preparative use of pure PPTases to stoichiometrically load phosphopantetheine onto heterologously expressed constructs containing PCP domains is the study of peptide bond-forming steps that occur between two covalently tethered aminoacyl-S-enzyme domains, the peptidyl-S-enzyme as donor to the downstream aminoacyl-S-PCP domain acting as nucleophilic partner in the condensation. Our initial effort to detect valyl self-transfer to yield a Val-Val-S-P-pant protein product was unsuccessful, either with the 143 kDa as donor and the 18-kDa fragment as acceptor or vice versa (data not shown). Selectivity may be imposed in several ways. For example, the donor to Val-SrfB1 may need to be the acylated tripeptidyl-S-SrfA3, where either or both the peptidyl (vs aminoacyl) moiety or the SrfA3/SrfB1 protein/protein recognition may be crucial determinants for efficient peptide bond formation. Expression of the double module SrfB1−SrfB2, a six-domain 300-kDa fragment, in *E. coli* (if soluble and phosphopantetheinylatable on both PCP domains) may allow interrogation of some of these specificity issues in peptide bond formation between two covalent acyl-S-enzyme intermediates. Finally, we have recently been able to use acylated CoA derivatives in place of CoA to convert apo-ACP to acylated holo-ACP domains using PPTases including Sfp (*17*). If, for example, Sfp would load an aminoacyl P-pant directly from an aminoacyl-CoA onto an apo-PCP domain, it may be possible to bypass eqs 1 and 2 and directly interrogate the specificity of peptide bond formation. We now have the tools to perform such experiments in the immediate future.

ACKNOWLEDGMENT

We are grateful to A. M. Gehring for preparation of EntB ArCP and Prof. M. Marahiel (Phillips Universität Marburg) for the gift of TycA PCP.

REFERENCES

1. Kleinkauf, H., and von Döhren, H. (1996) *Eur. J. Biochem. 236*, 335−351.
2. Walsh, C. T., Gehring, A. M., Weinreb, P. H., Quadri, L. E. N., and Flugel, R. S. (1997) *Curr. Opin. Chem. Biol. 1*, 309−315.
3. Stein, T., Vater, J., Kruft, V., Otto, A., Wittmann-Liebold, B., Franke, P., Panico, M., McDowell, R., and Morris, H. R. (1996) *J. Biol. Chem. 271*, 15428−15435.

4. de Crécy-Lagard, V., Marlière, P., and Saurin, W. (1995) *C. R. Acad. Sci. Paris 318*, 927−936.
5. Weber, G., Schorgendorfer, K., Schneider-Scherzer, E., and Leitner, E. (1994) *Curr. Genet. 26*, 120−124.
6. Rusnak, F., Sakaitani, M., Drueckhammer, D., Reichert, J., and Walsh, C. T. (1991) *Biochemistry 30*, 2916−2927.
7. Crosby, J., Sherman, D. H., Bibb, M. J., Revill, W. P., Hopwood, D. A., and Simpson, T. J. (1995) *Biochim. Biophys. Acta 1251*, 35−42.
8. Lambalot, R. H., Gehring, A. M., Flugel, R. S., Zuber, P., Lacelle, M., Marahiel, M. A., Reid, R., Khosla, C., and Walsh, C. T. (1996) *Chem. Biol. 3*, 923−936.
9. Lambalot, R. H., and Walsh, C. T. (1995) *J. Biol. Chem. 270*, 24658−24661.
10. Gehring, A. M., Bradley, K. A., and Walsh, C. T. (1997) *Biochemistry 36*, 8495−8503.
11. Nakano, M. M., Corbell, N., Besson, J., and Zuber, P. (1992) *Mol. Gen. Genet. 232*, 313−321.
12. Borchert, S., Stachelhaus, T., and Marahiel, M. A. (1994) *J. Bacteriol. 176*, 2458−2462.
13. Fuma, S., Fujishima, Y., Corbell, N., D'Souza, C., Nakano, M. M., Zuber, P., and Yamane, K. (1993) *Nucleic. Acids Res. 21*, 93−97.
14. Nakano, M. M., Marahiel, M. A., and Zuber, P. (1988) *J. Bacteriol. 170*, 5662−5668.
15. Nakano, M. M., Magnuson, R., Myers, A., Curry, J., Grossman, A. D., and Zuber, P. (1991) *J. Bacteriol. 173*, 1770−1778.
16. Cosmina, P., Rodriguez, F., de Ferra, F., Grandi, G., Perego, M., Venema, G., and van Sinderen, D. (1993) *Mol. Microbiol. 8*, 821−831.
17. Quadri, L. E. N., Weinreb, P. H., Lei, M., Nakano, M. M., Zuber, P., and Walsh, C. T. (1998) *Biochemistry, 37*, 1585−1595.
18. Stachelhaus, T., Hüser, A., and Marahiel, M. A. (1996) *Chem. Biol. 3*, 913−921.
19. D'Souza, C., Nakano, M. M., Corbell, N., and Zuber, P. (1993) *J. Bacteriol. 175*, 3502−3510.
20. Vater, J., Stein, T., Vollenbroich, D., Kruft, V., Wittman-Liebold, B., Franke, P., Liu, L., and Zuber, P. (1997) *J. Prot. Chem. 16*, 557−563.
21. Marahiel, M. A., Stachelhaus, T., and Mootz, H. (1997) *Chem. Rev. 97*, 2651−2673.
22. Vollenbroich, D., Mehta, N., Zuber, P., Vater, J., and Kamp, R. M. (1994) *J. Bacteriol. 176*, 395−400.
23. Stachelhaus, T., and Marahiel, M. A. (1995) *J. Biol. Chem. 270*, 6163−6169.
24. Vater, J., Mallow, N., Gerhardt, S., Gadow, A., and Kleinkauf, H. (1985) *Biochemistry 24*, 2022−2027.
25. Reichert, J., Sakaitani, M., and Walsh, C. T. (1992) *Protein Sci. 1*, 549−556.
26. MacCabe, A. P., van Liempt, H., Palissa, H., Unkles, S. E., Riach, M. B., Pfeifer, E., von Döhren, H., and Kinghorn, J. R. (1991) *J. Biol. Chem. 266*, 12646−12654.
27. Conti, E., Stachelhaus, T., Marahiel, M. A., and Brick, P. (1997) *EMBO J. 16*, 4174−4183.
28. Vater, J., Schlumbohm, W., Salnikow, J., Irrgang, K.-D., Miklus, M., Choli, T., and Kleinkauf, H. (1989) *Biol. Chem. Hoppe-Seyler 370*, 1013−1018.

BI9719859